

Substrate-Integrated Octave-Tunable Comblines Bandstop Filter with Surface Mount Varactors

Akash Anand, Yuhao Liu, and Xiaoguang Liu

Department of Electrical and Computer Engineering, University of California Davis, USA
 akaanand@ucdavis.edu, yuhliu@ucdavis.edu, and lxgliu@ucdavis.edu

Abstract—This paper presents an octave-tunable two-pole bandstop filter with tuning range of 0.56–1.18 GHz (2.1:1 tuning ratio). The bandstop filter is designed with two highly loaded comblines resonators with surface mounted solid state varactors. Theoretical analysis and modeling along with full wave simulation is presented in agreement with measured data. The measured peak attenuation in the stopband is approximately 27 dB at 1.18 GHz and is approximately 7 dB at 0.56 GHz. However, a minimum attenuation of at least 10 dB is maintained above 0.65 GHz (1.82:1 tuning ratio).

Index Terms—comblines filter, comblines resonator, evanescent-mode design, filter design, filters, full-wave simulation, measurement and modeling, modeling, tunable filters, tunable resonators, waveguide filters

I. INTRODUCTION

RF/microwave bandstop filters (BSFs) are essential components for rejecting unwanted signals. A tunable bandstop filter (BSF) allows for more flexibility in conventional microwave systems and is required in the recent growing interest of reconfigurable and dynamic RF/microwave systems. For example, tunable BSFs can reject unwanted or leaked signals coming into a reconfigurable receiver. When integrated in systems with non-linear devices, BSFs can suppress unintentionally generated signals, such as higher order harmonics in power amplifiers [1].

The peak attenuation level of a BSF depends heavily on the unloaded quality factor (Q_u) of the filter. For this reason, high Q_u 3-D comblines evanescent-mode (EVA) resonators were used to design BSFs in [2], [3]. In [2], a two-pole EVA BSF filter was presented using piezoelectric actuators with a tuning ratio of 1.12:1. To extend the tuning range, six piezoelectric actuator resonators were cascaded together in [3]. This topology achieved a tuning ratio of 7.8:1 when all six resonators were tuned to independent frequencies.

Simpler BSF topologies on planer structures with lumped elements as tuners have also been demonstrated [4]–[7]. In [4], the BSF tuned from 470 MHz to 730 MHz (1.55:1 tuning ratio) and maintained a stopband attenuation better than 16 dB. A stopband attenuation better than 50 dB was accomplished in [5] with a tuning range of 665–1000 MHz (1.5:1 tuning ratio). Additionally, other planer structures have demonstrated extended tuning range. For instance, a bi-directionally tuned end-loaded quarter-wave BSF was proposed for better tuning ratio than a conventional quarter wave BSF [6]. To achieve octave tuning, results from [7] show a BSF with lumped elements operating from 20 MHz to 55 MHz.

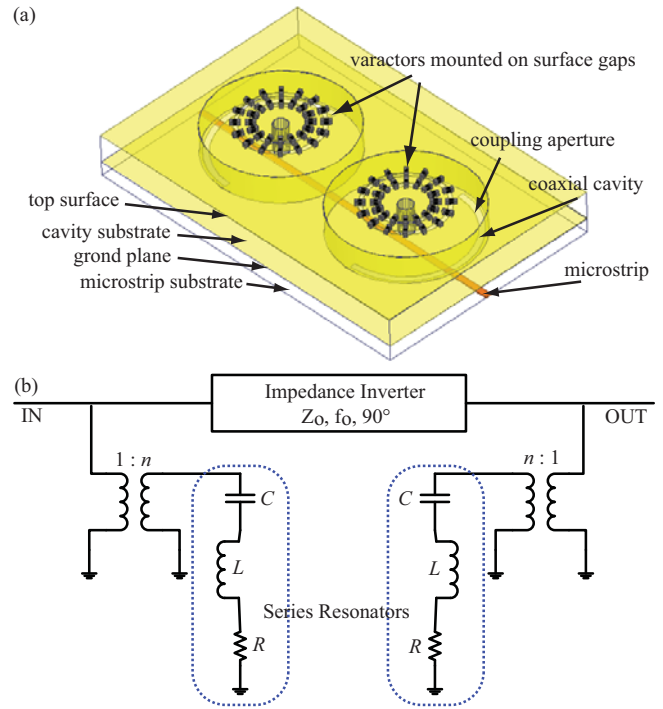


Fig. 1. (a) Proposed two-pole BSF and (b) lumped-distributed model for a two-pole BSF. Energy is coupled into the two series resonators through ideal transformers separated by an impedance inverter with an electrical length of 90° at f_o .

This work presents a BSF with surface mount lumped elements on a 3-D structure (see Fig. 1(a)). Compared to other 3-D filters such as [2], [3], planar surface mounted topologies allows for a reduced complexity in fabrication and assembly [9]–[11]. Yet the proposed structure maintains higher Q_u than planar microstrip topologies [10]. Measured results show tuning range above an octave from 0.56 GHz to 1.18 GHz using a two resonator topology (as opposed to the six used in [3]) and using varactors with tuning ratio of 4.2:1 (2.67–0.63 pF). The peak stopband attenuation ranges from 7 dB to 27 dB over the octave tuning range, but a minimum of 10 dB attenuation is maintained from 0.65 GHz to 1.18 GHz (1.82:1 tuning ratio).

II. DESIGN

A. Theoretical analysis

Fig. 1(b) shows a lumped-distributed model for a two-pole BSF [8]. Energy is coupled into two series resonators, with

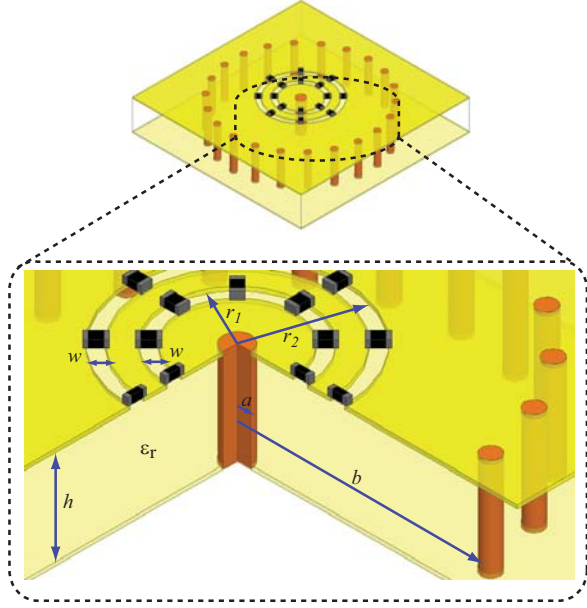


Fig. 2. Substrate-integrated combline resonator previously demonstrated in [10] with a close up view of the design parameters.

capacitance C , inductance L , and resistance R , through ideal transformers with $n:1$ ratio. An ideal impedance inverter, with characteristic impedance of Z_o and an electrical length of 90° at f_o frequency, separates the two coupled resonators.

In this work, the series resonators from Fig. 1 are realized by previously demonstrated octave tunable combline resonators loaded with lumped tuning elements [9], [10]. For convenience, this resonator structure is repeated in Fig. 2. A coaxial cavity is shorted at one end while two ring gaps are created on the other end, where lumped tuning elements (solid-state varactors) can be mounted over the gaps to tune the resonant frequency. With the guidelines suggested in [10], a resonator is designed with the dimensions given in Table I and label in Fig. 2. From the measured results in [10], a resonator with similar parameters achieved a Q_u of $\approx 180 - 200$ at 1.1 GHz with equivalent inductance of approximately $L = 3.31$ nH and equivalent capacitance of $C = C_v + C_o$, where C_v is the varactor capacitance and $C_o \approx 0.8$ pF is ring gap capacitance.

From

$$R = \frac{2\pi f L}{Q_u} \quad (1)$$

the extracted resistance (R) for the resonator with $Q_u \approx 180 - 200$ at $f = 1.1$ GHz is $R \approx 0.11 - 0.13 \Omega$. The lumped-distributed model in Fig. 1 is implemented in a circuit simulator (Advance Design System (ADS) [13]) with the extracted L , C , and R with ideal transformers ($n = 0.132$) and an ideal 50Ω transmission line with an electrical length of 90° at $f_o = 1$ GHz. Fig. 3 shows the simulation results for the tunable two-pole band stop filter with approximately 40 MHz BW as in Fig. 3 with ideal transformers. But if the BW changes, then stopband attenuation (S_{21}) will also change. For example, HFSS simulation in Fig. 5(b) shows that

TABLE I
DESIGNED RESONATOR PARAMETERS

resonator parameters	value
h	5 mm
b	12 mm
a	20 mils
w	0.3 mm
r_1	3 mm
r_2	4.2 mm
ϵ_r	3.27
varactors per ring	16

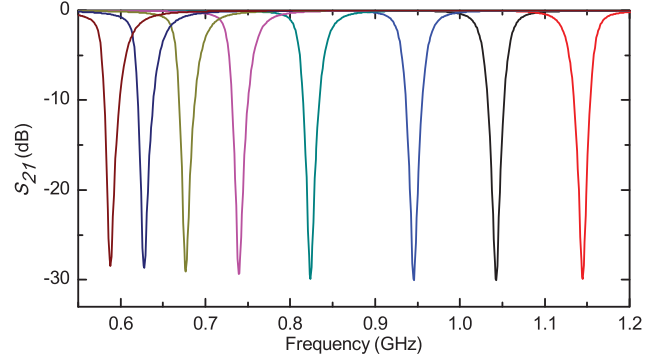


Fig. 3. Lumped-distributed model from Fig. 1 simulated in ADS with L , C , and R extracted from [10]. The BSF has a tuning range of $\approx 0.58 - 1.15$ GHz and maintains a 3-dB BW of ≈ 40 MHz.

B. Full-wave simulation

Fig. 4 shows the three main sections of the designed BSF (sections are separated for illustration). In the top section, varactors are mounted on the surface ring gaps (Fig. 4(a)). The middle section shows the two cavity resonators with coupling apertures on the ground plane to couple the energy into the resonators (Fig. 4(b)). The bottom section is a microstrip transmission line with the same coupling apertures in its ground plane as the resonators (Fig. 4(c)). Thus, energy is fed into the microstrip transmission line and coupled into the resonators via the apertures. The dimensions of the resonators are given in Table I and label in Fig. 2. The microstrip transmission line is designed to be 50Ω with the following dimensions: 20 mil substrate height, 1.108 mm microstrip width, and a dielectric constant of 3.27. The coupling apertures are separated by 4.6 cm to realize an electrical length of 90° at $f_o = 1$ GHz.

The coupling apertures represent the transformers in Fig. 1(b). Simulation from Ansys HFSS [12] in Fig. 5(a) shows that increasing ϕ (aperture size or n) in Fig. 4(c) increases the 3-dB fractional bandwidth (FBW) of the BSF: FBW increases from 2.4% (27 MHz) to 6.2% (67 MHz) when ϕ changes from 70° to 100° around 1.1 GHz. Note that the transformers used in ADS simulation from Fig 1(b) are ideal but the apertures are not ideal: the amount of coupling (n) depends on the frequency. Thus the absolute BW will change over the frequency range instead of maintaining a constant. If the BW changes, then stopband attenuation (S_{21}) will also change. For example, HFSS simulation in Fig. 5(b) shows that

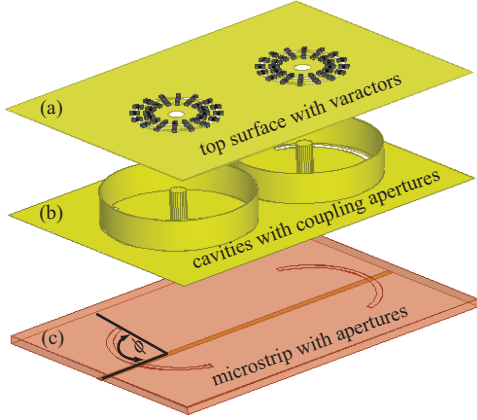


Fig. 4. Designed two-pole BSF (separated into three sections for illustration) with (a) the top section showing the surface mount varactors (b) middle section showing the two resonators with the coupling apertures and (c) bottom section showing a microstrip transmission line with identical coupling structures as the resonators.

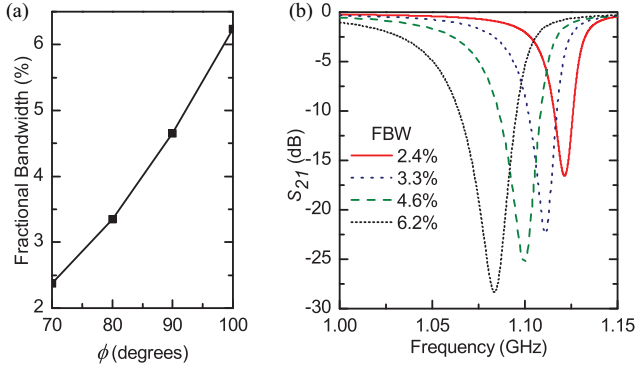


Fig. 5. HFSS simulation of (a) 3-dB FBW versus ϕ and the corresponding (b) S_{21} around 1.1 GHz. Note the slight decrease in frequency as the parasitic inductance and capacitance increase with larger aperture size (larger ϕ or FBW) [14].

as FBW is reduced from 6.2% to 2.4%, stopband attenuation worsens from $S_{21} \approx -28$ dB to $S_{21} \approx -17$ dB. Shifts in center frequency are observed due to parasitic capacitance and inductance introduced by the varying aperture size [14].

III. EXPERIMENTAL VALIDATION

Figs. 6(a) and (b) show the top and bottom view of the fabricated 50 Ω microstrip transmission line on a Rogers TMM3 substrate with the same dimension as previously used in HFSS simulation to realize an impedance inverter at 1 GHz. Fig. 6(c) shows the top view of the fabricated resonators with Skyworks SMV1405 varactors. Each varactor has a capacitance of $C_v = 0.63\text{--}2.67$ pF when biased from 0–30 V with an estimated series resistance of 0.8 Ω . The resonators are also fabricated on a Rogers TMM3 board with plated vias (≈ 1 mm diameter and < 2.5 mm spacing) forming the walls of the cavity. Dimensions of the resonators are given in Table I and labeled in Fig. 2. Figs. 6(b) and (d) show coupling apertures designed to give a 4.5% FBW or 45 MHz absolute BW around 1.1 GHz with ϕ of 90° (Fig. 5(a)). Figs. 6(e) and (f) show the top and bottom views of the assembled BSF:

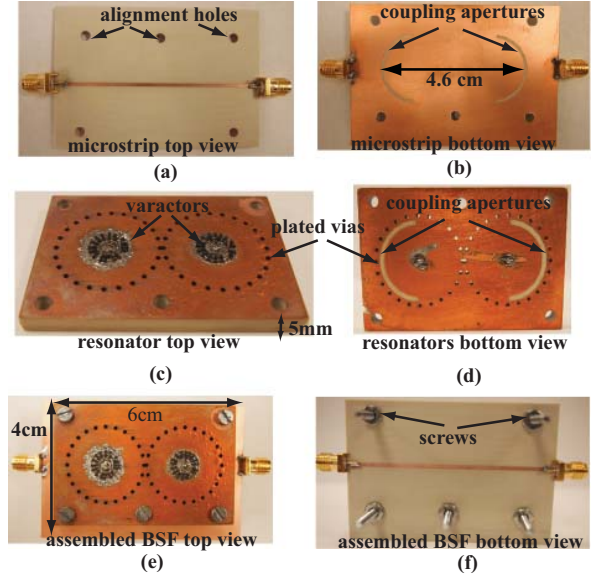


Fig. 6. Fabricated microstrip boards (a) top view and (b) bottom view with aperture spacing of 4.6 cm. (c) Top view of fabricated resonators with Skyworks SMV1405 varactors on the two ring gaps and (d) bottom view of the fabricated resonators with the coupling apertures. Both the microstrip board and resonators have identical alignment holes so they can be screwed together with the apertures back to back. (e) Top and (f) bottom view of assembled BSF.

the apertures on the microstrip board and the resonators are aligned together back-to-back and the two pieces are screwed together. The fabricated BSF is ≈ 6 cm \times 4 cm \times 0.5 cm by volume.

Figs. 7(a) and (b) show the measured S_{21} and S_{11} of the BSF. The measured tuning range is from 0.56 GHz to 1.18 GHz with FBW ranging from 4.2% at 1.18 GHz to 1.59% at 0.56 GHz. As explained in section II, the coupling aperture does not model an ideal transformer: as the frequency decreases, the wavelength increases relative to the aperture size and the coupling decreases, reducing FBW. As a result, instead of having a 40 MHz constant BW and more than 25 dB attenuation over the tuning range as in the theoretical simulation in Fig. 3, the measured stopband has a 42 MHz absolute BW and 27 dB stopband attenuation at 1.18 GHz but a reduced absolute BW of 9 MHz and stopband attenuation of 7 dB at 0.56 GHz. The measured tuning range compares well with theoretical results in Fig. 3, but the stopband attenuation cannot be directly compared since the BWs are not the same.

To extract Q_u , the transformer ratio n and resistance R in the lumped-distributed model in Fig. 1 are adjusted accordingly to match the measured BW and stopband attenuation. Thus with $L = 3.31$ nH and $R = 0.14$ Ω , Fig. 8 shows that ADS simulation with $C_v \approx 0.54$ pF and $n \approx 0.132$ pF, $C_v \approx 1.29$ pF and $n \approx 0.081$ pF, and $C_v \approx 2.9$ pF and $n \approx 0.053$ pF results in stopband center frequencies of 1.18 GHz, 0.84 GHz and 0.56 GHz. ADS simulation now shows the same BW and stopband attenuation as measured results in Fig. 8. Measured Q_u is then extracted from Eqn. 1: $Q_u \approx 177$ at 1.18 GHz, $Q_u \approx 120$ at 0.84 GHz, and $Q_u \approx 82$

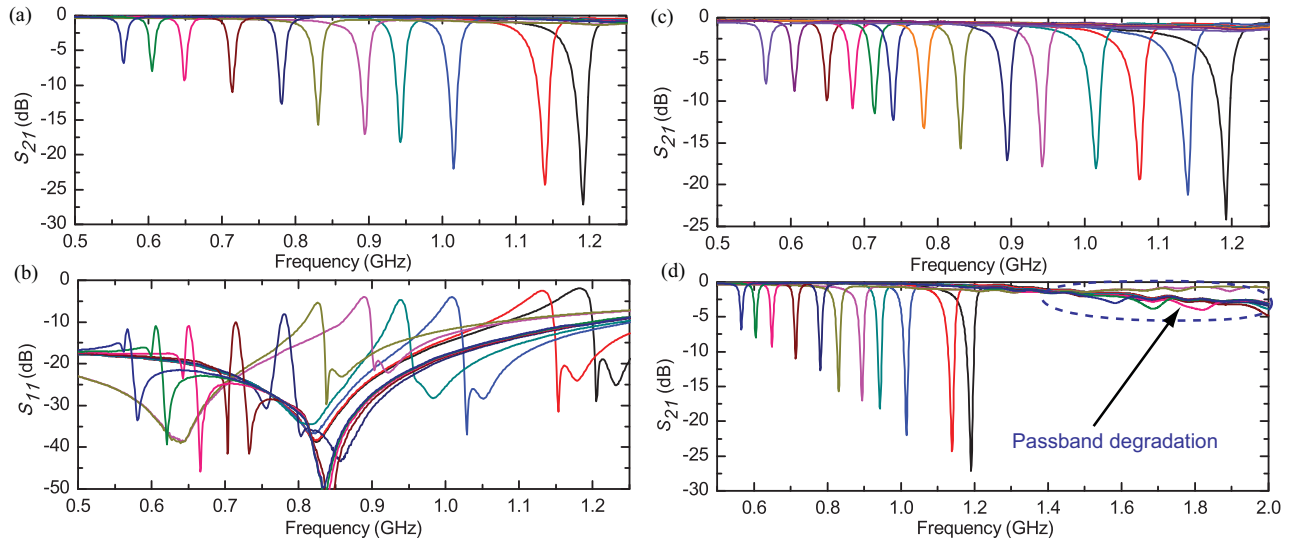


Fig. 7. (a),(b) Measured S-parameters for the BSF with an impedance inverter designed at 1 GHz and (c) 0.7 GHz. (d) Degradation in the passband is observed above 1.3 GHz due to the coupling apertures [3].

at 0.56 GHz, which are close to the expected range for the resonators in [10].

Another reason for worsened stopband attenuation at the lower frequencies is because the impedance inverter is optimal around 1 GHz. Fig. 7(c) shows a slight improvement in attenuation level at lower frequencies with the impedance inverter designed at 0.7 GHz. For example, the measured peak attenuation is ≈ 8 dB at 0.56 GHz instead of ≈ 7 dB, however the peak attenuation worsens by ≈ 3 dB at higher frequencies. Fig. 7(d) extends the frequency range from Fig. 7(a) to 2 GHz. Degradation in the passband is observed above 1.3 GHz due to the coupling apertures [3].

IV. CONCLUSION

This work presents an octave tunable BSF with lumped tuning elements. Theoretical modeling and HFSS simulation used to design the BSF show good agreement with measured response. The designed BSF has a tuning range of 0.56–1.18 GHz with attenuation levels ranging from 7 dB to 27 dB. A 10-dB minimum attenuation is achieved beyond 0.65 GHz and Q_u of 177 is extracted at 1.18 GHz.

REFERENCES

- [1] H. W. Liu, F. Tong, and X. Li, "Asymmetrical Spurline Resonator Design and its Application to Power Amplifiers," in *Art of Miniaturizing RF and Microwave Passive Components*, Dec. 2008, pp. 149-152.
- [2] T. Snow, J. Lee, and W. Chappell, "Tunable High Quality-Factor Absorptive Bandstop Filter Design," in *IEEE MTT-S Int. Microwave Symp. Digest*, Jun. 2012, pp. 1-3.
- [3] E. Naglich, J. Lee, D. Peroulis, and W. Chappell, "Extended Passband Bandstop Filter Cascade with Continuous 0.85-6.6 GHz Coverage," *IEEE Trans. Microw. Theory Tech.*, vol. 60, no. 1, pp. 21-30, Jan. 2012.
- [4] Y. C. Ou and R. Rebeiz, "Lumped-Element Fully Tunable Bandstop Filters for Cognitive Radio Applications," *IEEE Trans. Microw. Theory Tech.*, vol. 59, no. 10, pp. 2461-2468, Oct. 2011.
- [5] A. C. Guyette, "Intrinsically Switched Varactor-Tuned Filters and Filter Banks," *IEEE Trans. Microw. Theory Tech.*, vol. 60, no. 4, pp. 1044-1056, April 2012.

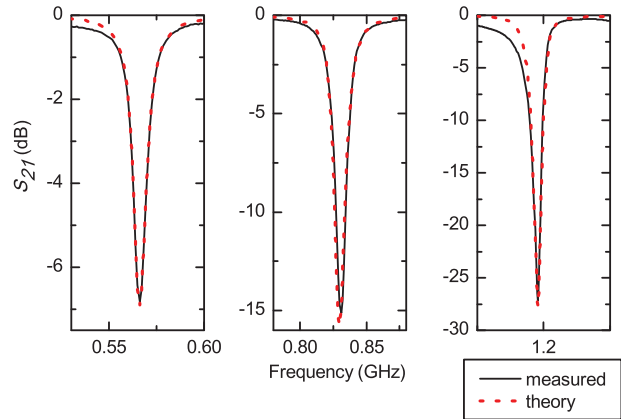


Fig. 8. To extract measured Q_u , n and R in Fig. 1(b) are adjusted accordingly in ADS simulation to match the measured response at three different frequencies.

- [6] Y. Ma, W. Che, J. Mao, and J. Chen, "Novel Tunable Bandstop Filters Using End-Loaded Quarter-Wavelength Resonators," in *Microw. and Millimeter Wave Techno.*, May. 2012, pp. 1-4.
- [7] D. R. Jachowski, "Octave Tunable Lumped-Element Notch Filter," in *IEEE MTT-S Int. Microwave Symp. Digest*, Jun. 2012, pp. 1-3.
- [8] I. C. Hunter, J. D. Rhodes, "Electronically Tunable Microwave Bandstop Filters," *IEEE Trans. Microw. Theory Tech.*, vol. 30, no. 9, pp. 1361-1367, Sep. 1982.
- [9] A. Anand et al., "A Novel High- Q_u Octave-Tunable Resonator with Lumped Tuning Elements," in *IEEE MTT-S Int. Microwave Symp. Digest*, Seattle, WA, June 2013.
- [10] A. Anand, J. Small, D. Peroulis, and X. Liu, "Theory and Design of Octave Tunable Filters with Lumped Tuning Elements," *IEEE Trans. Microw. Theory Tech.*, vol. 61, no. 12, pp. 4353-4364, Dec. 2013.
- [11] S. Sirci et al., "Varactor-Loaded Continuously Tunable SIW Resonator for Reconfigurable Filter Design," in *Proc. 41th. Eur. Microw. Conf.*, Oct. 2011, pp. 436-439.
- [12] Ansoft Cooperation, *High Frequency Structure Simulator*. [Online]. Available: <http://www.ansoft.com/products/hf/hfss/>
- [13] Agilent Technologies, *Advance Design Systems*. [Online]. Available: <http://www.home.agilent.com/agilent/>
- [14] J. S. Hong and B. Karyamapudi, "A general circuit model for defected ground structures in planar transmission lines," *IEEE Microw. Wireless Compon. Lett.*, vol. 15, no. 10, pp. 706-708, Oct. 2005.